Earth and Planetary Science Letters, 25 (1975) 93–102

EAST PACIFIC RIDGE (2°S–19°S) VERSUS NAZCA INTRAPLATE VOLCANISM: RARE-EARTH EVIDENCE

J.-G. SCHILLING

Graduate School of Oceanography, University of Rhode Island
Kingston, R.I. (U.S.A.)

and

E. BONATTI

Lamont-Doherty Geological Observatory of Columbia University, Palisades, N.Y. (U.S.A.)

Received May 9, 1974
Revised version received December 6, 1974

Basalts from seamounts within the Nazca Plate representing intraplate volcanism, and the East Pacific Ridge between 19°S and 2°N have similar light rare earth depleted abundance patterns. Both intraplate and ridge basalts appear to have been derived from the low-velocity layer apparently depleted in large lithophile elements (DLVL). Nepheline-normative basalts and ferrobasalts occasionally occurring on the East Pacific Rise are shown to have also been derived from the same DLVL source. Furthermore, the rare-earth pattern similarity of nepheline-normative and tholeiitic basalts from the East Pacific Rise is best explained by distinct, pressure induced, conditions of partial melting of the DLVL source; whereas total rare-earth pattern enrichment and relative europium depletion of the ferrobasalts are consistent with shallow depth fractional crystallization during ascent.

1. Introduction

Two main types of submarine volcanism have been recognized in the Pacific [1,2]; namely, fissural volcanism along the mid-ocean ridge and central-type volcanism in seamounts, often grouped in chains and occasionally emerging as islands. Since the acceptance of the sea-floor spreading theory [3], the origin of seamounts and branching volcanic chains has commonly been linked to mid-ocean ridges and their evolution. Menard has suggested that seamounts grow gradually while drifting away from the axis of the East Pacific Ridge (EPR) [4]. The mean life growth is of the order of a few million years; but the source of lava that a volcano continues to tap as it moves was not specified. The sources could either be as magma chambers trapped within the lithosphere, or deeper, within the asthenosphere. Aumento has suggested that pairs of seamounts equally spaced on opposite sides of the Mid-Atlantic Ridge started as single volcanoes at the crest and were subsequently split and separated [5]. Furthermore, Aumento also noted that across the MAR at 45°N, basalts from the summits of seamounts become progressively more alkaline and more silica-deficient the further they have receded from the ridge crest [5]. McBirney and Gass had earlier reported a similar pattern for volcanic islands [6]. Finally, Engel et al. [7] suggested that elevated volcanic edifices are generally alkalic due to vertical differentiation. These and other studies have led to the generalization customarily found in recent literature, that seamounts away from ridge axis tend to be alkalic.

Models relating distance from the ridge with either increasing size and elevation of the seamounts, extent of fractional crystallization or weathering of the lavas, or decreasing geothermal gradients, and as a result, increasing depth of partial melting, have been constructed to explain this increase in alkalinity of seamounts with distance from ridge axis [6,8].

These studies tend to overshadow the possibility that off-ridge or intraplate volcanism may be a more

* On leave from Rosenstiel School of Marine and Atmospheric Sciences, University of Miami, Miami, Florida 33149.

common phenomenon than so far realized. Few and obvious cases of large intraplate outpouring of lava such as Hawaii, the Galapagos or Reunion, have been attributed to mantle plumes [9,10] ; but attributing such an origin to any intraplate volcanism would be unwarranted.

In an extensive survey of rare-earth (RE) content in mid-ocean ridge basalts, Schilling concluded that normal mid-ocean ridge basalts are derived from a worldwide circling upper-mantle layer characteristically depleted in the light RE and other large lithophile elements (K, Rb, Cs, Sr, Ba) [11] . This layer has been called the depleted low-velocity layer (DLVL). Because of the apparent widespread nature of this mantle source for mid-ocean ridge basalts, there is a distinct possibility that some intraplate volcanism might also take source in the DLVL.

Bonatti and Fisher have shown that basalt from isolated seamounts within the Nazca Plate (Fig. 1) do not differ petrochemically from basalts erupted at the EPR axis, thus suggesting similar conditions of magma generation in the two cases [12]. Because of the definitely younger age of these seamount basalts relative to the surrounding sea floor [13,14], it was implied that these basalts could not have been emplaced originally on the East Pacific Ridge, nor on the fossil Galapagos Ridge which is postulated to have become inactive about 9–10 m.y. ago [15] . Furthermore, as seamounts appear not to be associated with any major structural feature (except perhaps P6702-23 which is close to a fracture zone – R.N. Anderson, personal communication), Bonatti and Fisher concluded that these seamounts represent intraplate volcanism [12] .

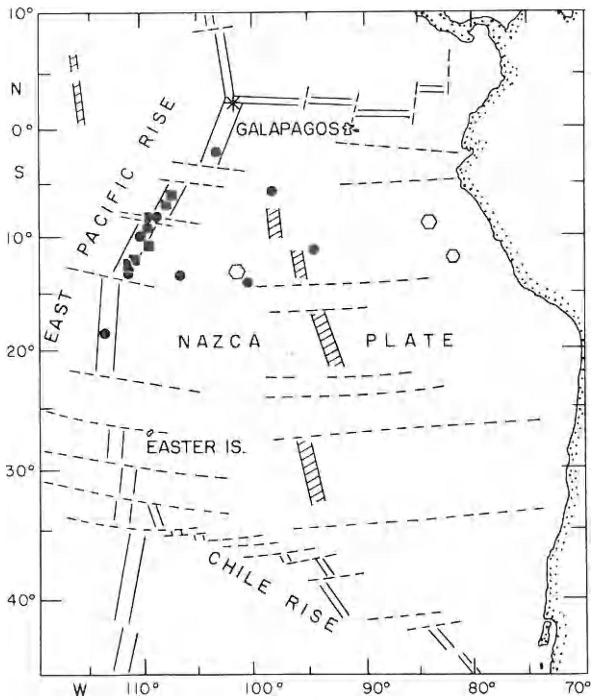

Fig. 1. Location of dredged basalts analyzed for rare earths. Circles indicate olivine tholeiite; squares, nepheline normative basalt. Star is a tholeiite from the West Galapagos Rift zone (to be published). Large hexagons indicate DSDP Leg 34 sites. Tectonic map is adapted from Herron [15]. Hatched areas represent remnant of the Galapagos Rise.

To further elucidate the origin of the Nazca Plate seamounts, we now report results on the distribution of RE in basalts from these seamounts. The RE data is consistent with Bonatti and Fisher's contention of a similar genesis for the Nazca intraplate and EPR basalts and suggests that both types of volcanism were apparently derived from the DLVL source in the upper mantle.

2. Normative petrology

Although the petrology of these rocks will be discussed in detail elsewhere [16] , a minimum presentation is required for discussing the RE results. The Fe_2O_3, FeO and $\Sigma FeO/MgO$ contents of the basalts are given in Table 1. The CIPW norms of the basalts studied for RE are presented in Fig. 2 on the Ne–Ol–Di–Hy–Oz tetrahedron of Yoder and Tilley [17] . The norms were calculated using a fixed 1.0% Fe_2O_3 content rather than measured values. This facilitates comparison of submarine basalts which may have suffered variable extent of alteration while exposed to seawater and possible hydrothermal alteration (see refs. [18,19] for a more detailed discussion of the problem and procedures to alleviate it). The net effect of this procedure on the present rock suite is to significantly reduce the normative scatter (Fig. 2). On this basis, the majority of basalts from the East Pacific Ridge and Nazca Plate seamounts plot across the olivine tholeiite field toward the field containing normative nepheline (Fig. 2). Five samples are slightly nepheline normative (samples C, F, J, L and N in Table 1). One is from an intraplate seamount (sample

TABLE 1

Rare-earth concentrations (ppm) determined by an instrumental neutron activaton analysis using a Ge(Li) detector (analyst R. Kingdey). P6702-44 and D-4 were also analyzed by Kay et al. [19], using a mass spectrometric technique. There is good agreement between the techniques. An average of 12 replicate analyses of rock standard BCR-1 is indicated for estimation of the precision and accuracy of the RE analytical technique used.

Code	Sample[1]	Normative rock type[2]	La	Ce	Nd	Sm	Eu	Tb	Dy	Tm	Yb	Lu	$[La/Sm]_{E.F.}$	Fe_2O_3	FeO	$\Sigma FeO/MgO$[3]
A	P6702-10	ol.tholeiite	3.3	–	–	3.2	1.4	–	4.9	–	3.1	0.44	0.73	1.86	6.80	1.02
B	P6702-20[4]	ol.tholeiite	2.2	–	–	2.9	1.1	–	4.7	–	–	0.34	0.52	3.00	5.77	1.10
C	P6702-23[4]	ol.tholeiite	3.8	–	–	4.3	1.5	–	6.4	–	3.3	0.52	0.62	4.61	5.65	1.48
D	P6702-25[4]	ol.tholeiite	3.4	–	–	3.6	1.2	0.92	5.0	–	2.4	0.46	0.66	3.46	5.88	1.16
E	P6702-27	ol.tholeiite	4.0	–	–	4.7	1.7	1.0	6.4	–	3.1	0.71	0.60	1.93	8.37	1.45
F	P6702-29	ne.basalt	4.3	–	–	4.1	1.4	1.03	–	–	2.8	0.50	0.72	0.76	7.90	1.05
G	P6702-32	ol.thol.(Fe-rich)	5.9	–	–	7.1	2.0	–	–	–	6.0	0.95	0.58	2.00	9.64	1.73
H	P6702-36	ol.tholeiite	1.5	–	–	2.9	1.2	–	4.3	–	2.8	0.41	0.35	2.00	7.08	1.08
I	P6702-39	ol.tholeiite	3.9	–	–	4.4	1.5	1.0	–	–	3.1	0.48	0.62	1.75	8.01	1.27
J	P6702-40	ne.basalt	3.2	–	–	4.1	1.6	0.94	–	–	3.6	–	0.55	1.36	7.88	0.91
K	P6702-42	ol.thol.(Fe-rich)	7.6	–	–	9.7	2.7*	–	12	1.2*	7.8	1.23*	0.55	4.17	11.33	2.91
L	P6702-44	ne.basalt	2.1	8.7*	8.4*	3.2	1.3*	0.82	5.6	0.52*	3.1*	0.45	0.45	2.11	7.82	1.21
M	P6702-50[4]	ol.tholeiite	3.5	–	–	3.4	1.3	0.92	5.1	–	2.1	0.36	0.72	2.04	7.24	1.22
N	Amph D-2	ne.basalt	4.2	13.8*	11.2*	3.9	1.5	0.95	6.2	0.47*	3.1*	0.44*	0.75	7.14	2.96	1.19
O	Amph D-3	ol.tholeiite	3.5	–	–	3.1	1.2	0.65	5.2	–	2.8	–	0.79	1.55	10.24	1.73
P	Amph D-4	ol.tholeiite	2.5	–	–	3.1	1.2	0.76	6.1	–	2.5	–	0.55	1.35	7.85	1.08
	BRC-1[5]	basalt std.	26.5			7.4	2.2	1.3			3.6	0.52				
			± 6.5%			±7.2%	±7.8%	±15%			±13.3%	±5.6%				

* Analyses obtained using a high resolution low energy Ge(Li) detector.

1 Sample locations and depths of collection are given in ref. [12].

2 Based on Yoder and Tilley [17] normative classification. Norms were calculated for a fixed 1% Fe_2O_3 and on a water-free basis.

3 ΣFeO is for total iron expressed as FeO wt.%.

4 Nazca Plate seamounts.

5 Average of 12 replicate analyses and percent standard deviation from the mean (1σ).

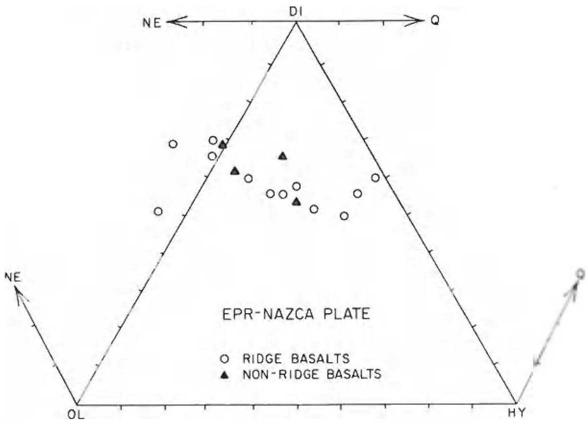

Fig. 2. Qz–Di–Hy–Ol–Ne diagram for the basalts analyzed for RE. The norms are from analyses recalculated with Fe_2O_3 = 1% and free of water. Analyses are from Bonatti et al. [16].

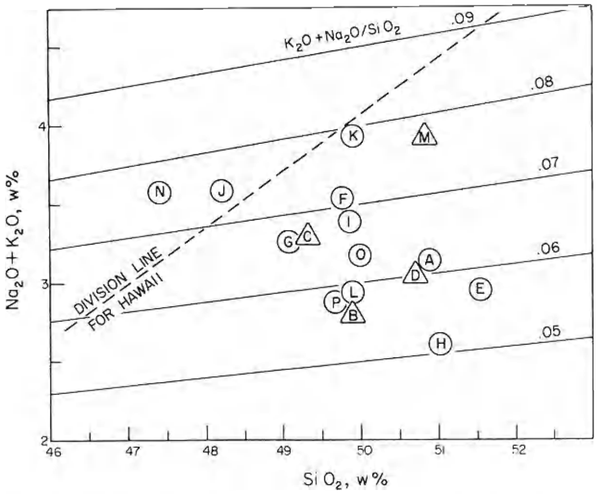

Fig. 3. Alkali–silica diagram for EPR basalts (circles) and Nazca intraplate seamount basalts (triangle). The empirical boundary between tholeiitic and alkaline basalts of Hawaii [21] is shown for comparison (dashed line). Family of thin lines are for constant $K_2O + Na_2O/SiO$ ratios. For a theoretical discussion of this diagram, see McBirney and Williams [34, pp. 128–129]. Data taken from ref. [16] and letter coding is listed in Table 1.

C), the other four are from the EPR (samples F, J and L). Sample N (Amph D2), with the highest nepheline-normative content, was dredged from a topographic high on the EPR crest, at a level shallower than that of the other EPR samples by about 1 km.

On the other hand, if measured Fe_2O_3 values are used to calculate the norms, samples F, J and N remain nepheline normative, samples C and L become hypersthene rather than nepheline normative (sample C is highly oxidized 4.7% Fe_2O_3, 5.8% FeO, 1.23% H_2O^+ and 0.53% H_2O^-), and samples K and E become slightly quartz normative rather than containing a small amount of normative olivine. The other samples remain within the olivine–hypersthene–diopside normative field of Fig. 2.

It would seem from Fig. 2, that among olivine tholeiites, the intraplate seamounts appear to plot closer to the olivine–diopside join. However, if additional samples analyzed for major elements, but not for rare earths, are included, no systematic distinction between EPR and Nazca intraplate seamount basalts can be made. They both range from the diopside–hypersthene join through olivine tholeiite and transitional basalts [20], to nepheline-normative basalts. Two noticeably Fe-rich lavas, which are also higher in total rare-earth content (samples G and particularly K with respectively 11.5 and 15.3% total iron expressed as FeO), are on a normative basis indistinguishable from other olivine tholeiites.

The extent to which the normative scatter of these basalts reflects the primary composition of the magma rather than deuteric or low-temperature alteration remains uncertain. Analyses of the glass fraction of these basalts tend to plot closer to the Di–Hy join than those of the microcrystalline fraction, suggesting that some deuteric alteration and/or low-temperature alteration have occurred [16].

The degree of alkalinity of these rocks relative to silica is shown in Fig. 3, which for comparison only, also shows the two fields of alkali and tholeiitic lava series from the Hawaiian Islands as delineated by McDonald and Katsura [21]. Of the (5) nepheline-normative basalts discussed previously, only samples N and J are high in alkali (Na_2O mostly) relative to silica, samples C and F are relatively high, whereas sample L is comparable to the majority of EPR basalts. Of the (4) Nazca Plate seamounts, the alkalinity of samples B and D is rather low and similar to a good majority of the EPR basalts, sample C is relatively high but remains comparable to some EPR, and sample M is high in alkali content and similar to the EPR ferrobasalt K (but its total iron content is lower, 9.2% compared to 15.3% for sample K). In other words, the (4) Nazca Plate seamounts overlap with EPR basalts not only in normative content but also in alkalinity, relative to silica. Furthermore, it has also been previously emphasized that the Niggli quartz index of the (4) Nazca Plate seamounts and EPR basalts are comparable [12]. Finally, the EPR basalts N and J appear definitely higher in alkalis (relative to silica) than most EPR basalts, and of the two, N is definitely fresh, as also apparent from the FeO/Fe_2O_3 and H_2O^+ given above.

3. Rare-earth evidence

RE data for intraplate seamount basalts and for the East Pacific Ridge axial basalts are given in Table 1. An average of replicate RE analysis of rock standard BCR-1 is also given for estimation of the precision and accuracy of the instrumental neutron activation methods used. Despite the petrochemical variation among the basalts (Fig. 2), they are all light RE-depleted, whether derived at the ridge axis or as intraplate seamounts (Fig. 4). Although there is a tendency for the chondrite normalized $[La/Sm]_{E.F.}$ ratio to increase with increasing K_2O content, or K_2O/Na_2O ratio (Fig. 5a and b), the $[La/Sm]_{E.F.}$ still remains less than unity and again, the (4) Nazca Plate Seamounts and EPR basalts cannot be separated on this basis; nor can they be by considering the variation of La or $[La/Sm]_{E.F.}$ versus $\Sigma FeO/MgO$ ratio of the basalts. These later plots, using the relevant data of Table 1, would also show complete overlap between the Nazca Plate seamounts and the EPR basalts.

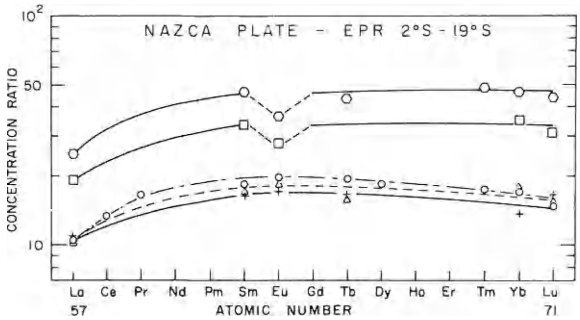

Fig. 4. Chondrite normalized rare-earth pattern of dredged basalts. Hexagon is for fractionated sample P6702-42 and square for P6702-32. Circles indicate average for EPR nepheline-normative basalts; triangles, average for EPR tholeiites, and crosses, average for Nazca Plate seamount basalts. Data is taken from Table 1.

Nepheline-normative basalts and tholeiitic basalts on the axis of the EPR have practically indistinguishable RE patterns which appear also to be unrelated to elevation: sample N (Amph D-2) is the most nepheline normative of the basalts and is derived from a topographic high over the ridge crest, yet its RE pattern is nearly indistinguishable from other Ne-normative or tholeiitic basalts of the ridge; its $[La/Sm]_{E.F.}$ is slightly higher than the other basalts but still remains less than one, thus light RE-depleted and comparable to other EPR basalts (Fig. 5a and b). The close occurrence of Ne-normative and tholeiitic basalts with nearly

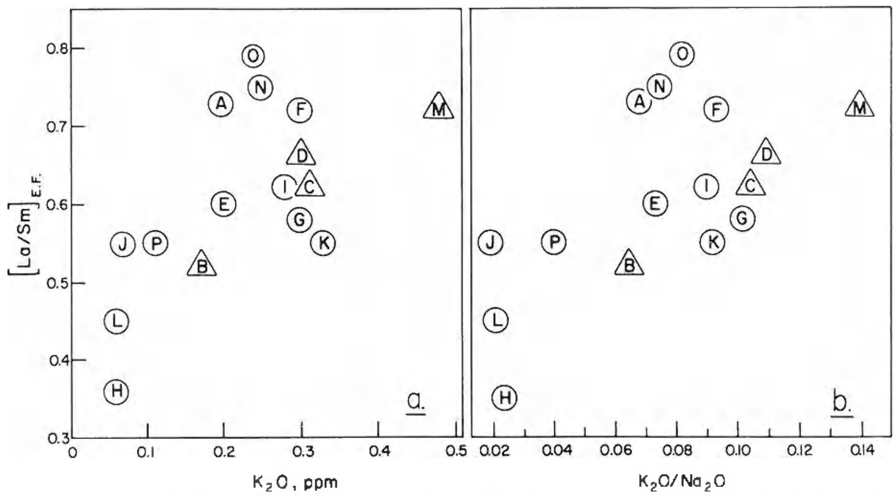

Fig. 5. Variation of chondrite normalized ratio $[La/Sm]_{E.F.}$ against (a) K_2O content, and (b) K_2O/Na_2O, for EPR basalts (circles), and Nazca intraplate seamount basalts (triangles). Note the rough positive correlation. Data taken from ref. [16] and letter coding is listed in Table 1.

identical RE is not unique to the EPR, but has also been observed from a single dredge haul on the Terceira Trough, Azores, by one of us (J-G.S.).Theoretically, nepheline-normative and tholeiitic-like melts with practically identical RE patterns can be obtained by the same extent of partial melting of a mantle source characterized by a unique RE pattern and composed of olivine, clinopyroxene, orthopyroxene and spinel, but by melting at different eutectic points within the same quartenary phase sytem [22]. This is because the relative proportions of the phases entering the melt (i.e. eutectic proportions) do not affect appreciably the RE composition of the melt produced by partial melting, other things being equal; whereas the primary phase proportions of the original mantle source and the degree of melting are indeed influential factors [22]. The different eutectic compositions required to produce the nepheline-normative and tholeiitic melts could then be considered to have been induced by distinct pressure conditions of partial melting (or depth of magma segregation), as suggested by Kushiro [23,24] . The model would satisfy both the major and the trace element chemistry. On the other hand, if distinct mantle mineralogy induced by pressure is invoked to satisfy the major element chemistry [25], rather ad hoc mantle RE composition(s) and extent(s) of partial melting would be required to produce the same RE patterns observed in the EPR nepheline-normative and tholeiitic basalts [22]. We prefer the first explanation.

Finally, the $[La/Sm]_{E.F.}$ of the two ferrobasalts K and G are also similar to other EPR basalts. However, the overall level of RE enrichment of ferrobasalts K and G is respectively ~1.5 and ~2.5 higher than the average RE pattern of the other EPR basalts studied (Fig. 4); and both ferrobasalts show an europium depletion to an extent proportional to their total enrichment in RE (Fig. 4 and Table 1.) A similar type of RE enrichment and fractionation was noted by Kay et al. [19] from a nearby locality (sample V21-40 in ref. [19]). The differentiation of such lava was shown to have been produced by extensive fractional crystallization of plagioclase and olivine at shallow depth [19]. These authors also emphasized that such extensive fractional crystallization, yielding Fe-rich differentiated melts, had little effect on the slope abundance pattern, in agreement with theoretical predictions [11] . On a $[La/Sm]_{E.F.}$ vs. $[Yb]_{E.F.}$ diagram discussed by Schilling [11,26], such differentiation would typically follow the olivine-gabbro fractionation trend which affects the $[La/Sm]_{E.F.}$ very little. Ferrobasalts G and K appear to have been produced by such shallow depth fractional crystallization, but to a lesser extent than as for generating the differentiated melt V21-40 reported by Kay et al. [19].

4. RE variation along the axis of the East Pacific Ridge

In Fig. 6, we plot $[La/Sm]_{E.F.}$ versus latitude along the axis of the East Pacific Ridge. The $[La/Sm]_{E.F.}$ remains remarkably constant along the EPR from 19°S to 2°N, at the triple junction of the EPR and the West Galapagos Rift zone (Hess Depression), thus over a distance of some 3000 km. No variation with elevation is apparent along the EPR axis; and the profile includes all normative types discussed earlier, that is: the common olivine tholeiites, the iron-rich derivative melts of rare occurrence, and the few nepheline-normative basalts.

Recently, Schilling [22] has subdivided mid-ocean ridges into segments of at least three different genetic kinds, namely: normal (NRS), transitional (TRS) and plume ridge segments (PRS). "Normal" mid-ocean ridge segments (NRS), to which the EPR segment between 19° to 2°N appears to belong, are characterized by normal ridge elevation, well developed and symmetrical magnetic anomaly lineaments, typical oceanic crustal thickness and structure [27], similar and uniform lithosphere subsidence characteristics apparently independent of spreading rates [28], and finally, greater seismicity than TRS, judging from the Reykjanes Ridge [29]. Sea-floor basalts derived from such segments are largely tholeiitic, depleted in large ionic lithophile elements, initially low in radiogenic isotopes, with $[La/Sm]_{E.F.} < 1$ and are passively derived from the "depleted low-velocity layer" (DLVL) in the asthenosphere, in response to the spreading.

On the other hand, ridge segments intersecting platforms underlain by rising plumes and their transition to normal ridge segments, have distinct geochemical and geophysical characteristics [22,30,31]. The light RE depletion of EPR basalts between 19°S and 2°N, the lack of latitudinal variation of the $[La/Sm]_{E.F.}$, and other geophysical characteristics

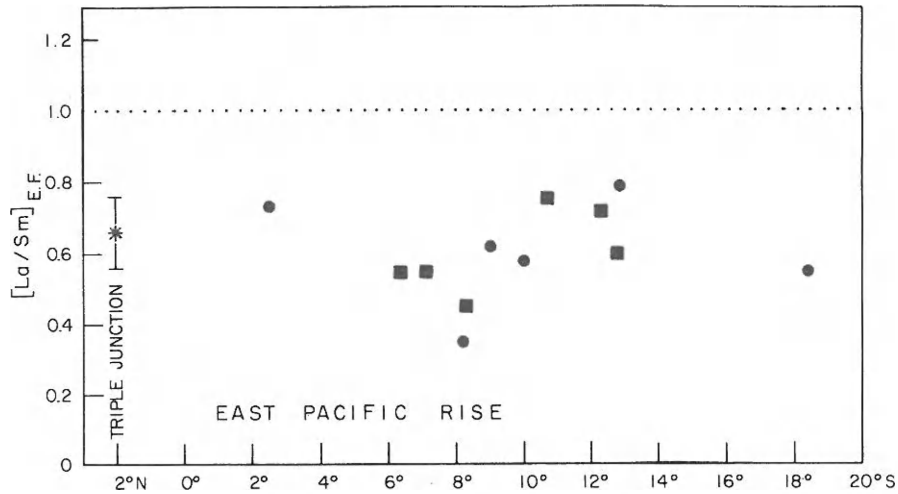

Fig. 6. Variation of chondritic normalized ratio $[La/Sm]_{E.F.}$ of dredged basalts with latitude along the East Pacific Ridge axis. Symbols are the same as in Fig. 1. Data taken from Table 1.

also concurrent [15], suggest that this segment of the East Pacific Rise represents indeed a "normal" ridge segment.

5. RE variation from the East Pacific Ridge and across the Nazea Plate

We now turn to RE variations across the Nazca Plate. Fig. 7 shows the $[La/Sm]_{E.F.}$ variation of the seamounts with distance from the EPR axis. The

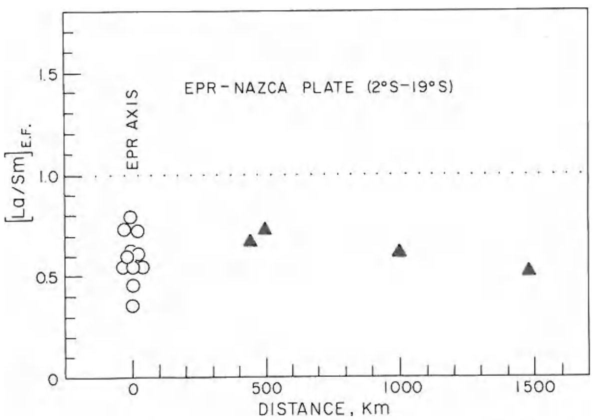

Fig. 7. Variation of chondritic normalized ratio $[La/Sm]_{E.F.}$ of dredged basalts with distance from the East Pacific Ridge, across the Nazca Plate. Data is taken from Table 1.

light-RE ratio stays practically constant from the EPR and outward.

It has recently been shown that the $[La/Sm]_{E.F.}$ of basalts can be considered as being representative of that of the mantle source from which such basalts are derived [22]. This is because the $[La/Sm]_{E.F.}$ of basaltic melts becomes increasingly similar to that of its mantle source as the degree of partial melting increases. Above some 20% of partial melting, which the EPR and Nazca Plate seamount basalts are probably the product of [25], the $[La/Sm]_{E.F.}$ is practically identical to its mantle source; and the ratio can reliably be used as an indicator of mantle sources. On this basis, the Nazca intraplate seamount basalts appear to have been derived from the same source as the EPR basalts, that is apparently from the DLVL. The RE results corroborate earlier findings revealing no systematic difference between the basalt chemistry of the EPR and Nazca Plate seamounts [12]. Furthermore, the RE data of these seamounts support the contention that these seamounts did not start forming on the East Pacific Ridge with subsequent growth from magma trapped within the lithosphere during plate drifting [12,14]. Some differentiation by fractional crystallization would be expected during such a cooling process, but is not apparent. Thus the seamounts must represent off-ridge volcanism intruding older sea floor and must have apparently grown by tapping the depleted low-velocity layer (DLVL) characteristically depleted in light-RE; providing, of course, that the age of these seamount basalts are indeed younger than the sea floor surrounding them, and this appears to be the case [13,14].

On this premise, the $[La/Sm]_{E.F.}$ uniformity across some 1600 km of the Nazca Plate also implies spatial RE uniformity of the DLVL over this area for the last few million years; thus adding new evidence for a rather worldwide extent and first order uniformity of the DLVL, as earlier suggested by one of us [11], and further substantiated recently [22].

As an additional point of interest, a plot of the relevant data from Table 1 would show that the heavy-RE fractionation pattern of the Nazca Plate seamount basalts B and M tends to have, relative to EPR basalts, a slightly more accentuated negative slope with increasing atomic number from Eu to Lu. The effect does not seem related directly to distance from the ridge axis. This small heavy-RE depletion can be modeled by involving garnet during equilibrium partial melting in the DLVL. This has recently been shown by considering partial melting in the following two simplified mantle systems, both characterized by the same total RE content and light-RE depleted pattern [22]. These are (1) $olivine_{60}$–$orthopyroxene_{25}$–$clinopyroxene_{15}$ (with or without a few percent of spinel), (2) $olivine_{60}$–$orthopyroxene_{16}$–$clinopyroxene_{12}$–$garnet_{12}$. The two mineral assemblages can respectively produce (1) the EPR basalts by some 30% partial melting at a eutectic point Ol_{25}–Opx_{20}–Cpx_{55}, and (2) the Nazca intraplate seamounts B and M by some 20% partial melting at a eutectic Ol_{03}–Opx_{03}–Cpx_{47}–Gar_{47}. In other words, conversion of clinopyroxene and/or orthopyroxene (and spinel) into garnet, yet keeping the olivine content and the primary mantle source RE pattern approximately constant, could account for the small negative heavy-RE fractionation slope of the Nazca intraplate seamount basalts B and M [22].

The above considerations could be interpreted as to suggest that the two Nazca intraplate basalts B and M were derived from an upper asthenosphere (DLVL) (or evolved in a lower lithosphere) characterized by a garnet facies mineralogy; and thus would have evolved somewhat deeper than at the ridge axis [25]. The model genesis for these two intraplate seamounts would be compatible with the Forsyth and Press [32] petrological models of a spreading and cooling lithosphere causing garnet to be stable near the base of the lithosphere, a few hundred kilometers away from the ridge crest. Although the possibility of garnet involvment for these two intraplate seamounts remains distinct, the above suggestion must be treated with caution as: (1) the effect observed on the heavy RE for sample B and M is indeed small and the distinction is further complicated by analytical uncertainties (see Table 1 for precision of the method used), (2) the effect is apparent only for two of the Nazca Plate seamounts studied and thus cannot be generalized, and (3) the computer modeling for the partitioning of the rare earths during partial melting offers no uniqueness of solution.

6. Conclusions

(1) The RE results on the Nazca Plate seamounts and bordering EPR support the earlier [12] conclusion that, at least in this region of the Pacific, conditions of intraplate magma generation are similar to those operating at the axis of a "normal ridge segment." Both intraplate and normal ridge basalts appear to have been derived from the depleted low-velocity layer, remarkably uniform in RE content, over an area beneath the Nazca Plate and its EPR boundary of at least the order of $3–4 \times 10^6$ km^2, and probably much more; as well as under partial melting conditions or not too dissimilar thermal regimes.

(2) The RE evidence on the Nazca intraplate seamount volcanism is in marked contrast to models for off-ridge seamount volcanism derived from magma reservoirs trapped within or near the base of a drifting lithosphere and intermittently feeding the overlying seamount, such as considered by Green's [33] Stage III model, or Aumento [8]. It is also in marked contrast to the concept of seamounts or islands growing over a drifting lithosphere and becoming increasingly more undersaturated further away from the ridge [5,6].

(3) The East Pacific Ridge between latitude 2°N and 19°S, including the triple junction with the West Galapagos Rift zone, can be considered as a "normal" ridge segment, in the sense defined above.

(4) The similar light-RE depleted pattern of both tholeiitic and nepheline-normative basalts from the EPR are best explained by partial melting of a compositionally and mineralogically relatively uniform

mantle (DLVL), but distinct, pressure-induced, eutectic compositions [23]; and thus reflect distinct local thermodynamical regimes, or depth of magma segregation, during the rise of mantle diapirs beneath the East Pacific Ridge.

(5) The iron-rich olivine tholeiites, also enriched in total RE, with depleted Eu, but having retained a light-RE depletion, represent most likely derivative melts of rare occurrence, produced at shallow depth by unusually extensive fractional crystallization of olivine and feldspar. Although apparently very infrequent, such iron enrichment and RE type of fractionation do reflect another characteristic process operating occasionally along "normal" ridge segments for reasons which remain to be deciphered.

Acknowledgements

We thank M. Murray, M. Zajac and R. Kingsley for help, and F. DiMeglio and his staff for neutron irradiations and facilities at RINSC. This work was supported by the U.S. National Science Foundation and ONR.

References

1 H.W. Menard, Marine Geology of the Pacific (McGraw-Hill, New York, 1964) chapter 4.
2 E. Bonatti, Mechanisms of deep-sea volcanism in the South Pacific, in: Researches in Geochemistry, 2 (Wiley, New York, 1967) 453.
3 F.J. Vine, Spreading of the ocean floor: new evidence, Science 154 (1966) 1405.
4 H.W. Menard, Growth of drifting volcanoes, J. Geophys. Res. 74 (1969) 4827.
5 F. Aumento, The Mid-Atlantic Ridge near 45°N, 2. Basalts from the area of Confederation Peak, Can. J. Earth Sci. 5 (1968) 1.
6 A.R. McBirney and I.G. Gass, Relations of oceanic volcanic rocks to mid-ocean rises and heat flow, Earth Planet. Sci. Lett. 2 (1967) 265.
7 A.E.J. Engel, C.G. Engel and R.G. Havens, Chemical characteristics of oceanic basalts and the upper mantle, Geol. Soc. Am. Bull. 76 (1965) 719.
8 F. Aumento, Magmatic evolution on the Mid-Atlantic Ridge, Earth Planet. Sci. Lett. 2 (1967) 225.
9 J.T. Wilson, Evidence from islands on spreading of ocean floors, Nature 197 (1963) 536.
10 W.J. Morgan, Convection plumes in the lower mantle, Nature 230 (1971) 42.
11 J-G. Schilling, Sea-floor evolution: rare-earth evidence, Phil. Trans. R. Soc. Lond. A268 (1971) 663.
12 E. Bonatti and D.E. Fisher, Oceanic basalts: chemistry versus distance from oceanic ridges, Earth Planet. Sci. Lett. 11 (1971) 307.
13 D.E. Fisher, Fission-track ages of deep-sea glasses, Nature 221 (1969) 549.
14 D.E. Fisher, E. Bonatti, O. Joensuu and J. Funkhouser, Ages of Pacific deep-sea basalts, and spreading of the sea-floor, Science 160 (1968) 1106.
15 E.M. Herron, Sea-floor spreading and the Cenozoic history of the East-Central Pacific, Geol. Soc. Am. Bull. 83 (1972) 1671.
16 E. Bonatti, D.E. Fisher, P. Kirst and R. Mazzuoli, Basalts from the East Pacific Rise and the Nazca Plate, to be submitted to Contrib. Mineral. Petrol. (1974).
17 H.S. Yoder and C.E. Tilley, Origin of basaltic magmas: an experimental study of natural and synthetic rock systems, J. Petrol. 3 (1962) 342.
18 J.R. Cann, Major element variations in ocean-floor basalts, Phil. Trans. Roy. Soc. Lond. A268 (1971) 495.
19 R. Kay, N.J. Hubbard and P.W. Gast, Chemical characteristics and origin of oceanic ridge volcanic rocks, J. Geophys. Res. 75 (1970) 1585.
20 M.N. Bass, Occurrence of transitional abyssal basalt, Lithos. 5 (1972) 57.
21 G.A. MacDonald and T. Katsura, Chemical composition of Hawaiian lavas, J. Petrol. 5 (1964) 82.
22 J-G. Schilling, Rare-earth variations across "normal segments" of the Reykjanes Ridge, 60°N–53°N, Mid-Atlantic Ridge, 29°S and East Pacific Rise, 2°S–19°S; and evidence on the composition of the underlying low-velocity layer, J. Geophys. Res. (1975) in press.
23 I. Kushiro, Compositions of magmas formed by partial zone melting of the earth's upper mantle, J. Geophys. Res. 73 (1968) 619.
24 I. Kushiro, Origin of some magmas in oceanic and circum-oceanic regions, Tectonophysics 17 (1973) 211.
25 D.H. Green and A.E. Ringwood, The genesis of basaltic magmas, Contrib. Mineral. Petrol. 15 (1967) 103.
26 J-G. Schilling, Iceland mantle plume, Nature 246 (1973) 141.
27 P.R. Vogt, E.D. Schneider and G.L. Johnson, The crust and upper mantle beneath the sea, in: The Earth's Crust and Upper Mantle, ed. P.J. Hart, Geophysical Monograph 13 (Am. Geophys. Union, Washington, D.C., 1969) 554.
28 J.G. Sclater, R.N. Anderson and M.L. Bell, Elevation of ridges and evolution of the Central Eastern Pacific, J. Geophys. Res. 76 (1971) 7888.
29 T.J.G. Francis, The seismicity of the Reykjanes Ridge, Earth Planet. Sci. Lett. 18 (1973) 119.
30 J-G. Schilling, Iceland mantle plume: geochemical evidence along Reykjanes Ridge, Nature 242 (1973) 565.
31 J-G. Schilling, Afar mantle plume: rare-earth evidence, Nature Phys. Sci. 242 (1973) 2.

32 D.W. Forsyth and F. Press, Geophysical tests of petrological models of the spreading lithosphere, J. Geophys. Res. 76 (1971) 7963.
33 D.H. Green, *Composition of basaltic magmas as indicators* of conditions of origin: application to oceanic volcanism, Phil. Trans. R. Soc. Lond. A268 (1971) 707.
34 A.R. McBirney and H. Williams, Geology and petrology of the Galapagos Islands, Geol. Soc. Am. Memoir 118 (1969) 1.